First-principles investigation of a bistable boron-oxygen interstitial pair in Si

A. Carvalho* and R. Jones
School of Physics, University of Exeter, Stocker Road, Exeter, EX4 4QL, United Kingdom

M. Sanati and S. K. Estreicher
Physics Department, Texas Tech University, Lubbock, Texas 79409-1051, USA

J. Coutinho
Department of Physics, University of Aveiro, Campus Santiago 3810-193 Aveiro, Portugal

P. R. Briddon
School of Natural Sciences, University of Newcastle upon Tyne, Newcastle upon Tyne, NE1 7RU, United Kingdom
(Received 21 March 2006; published 15 June 2006)

Local density functional calculations are used to predict and compare the properties of the two distinct interstitial boron-interstitial oxygen (B_iO_i) complexes recently reported in the literature. The electronic and free energies, as well as the small transformation barrier, suggest that both forms of the defect are present at the temperature at which the defect forms. The vibrational spectra of the defects are predicted. The electrical levels of the defect are calculated and compared to experimental data. The existence of two forms of the B_iO_i defect may have implications for the lifetime degradation of space-based Czochralski-silicon solar cells.

DOI: 10.1103/PhysRevB.73.245210 PACS number(s): 61.72.−y, 71.55.Cn, 65.40.Gr, 71.15.Mb

I. INTRODUCTION

Interstitial boron-oxygen ($\{B_i,O_i\}$) defects are believed to be responsible for the degradation of B-doped Czochralski-grown silicon (Cz-Si) solar cells exposed to radiation.[1] The formation of $\{B_i,O_i\}$ proceeds via a three-step process. Upon irradiation, intrinsic defects, such as Si self-interstitials, are produced. These interstitials are captured by substitutional boron (B_s) and result in the formation of fast-diffusing boron–self-interstitial (BI) complexes. Finally, BI complexes migrate through the lattice eventually reacting with the abundant interstitial oxygen centers.

A BI complex can be described as a nearly substitutional boron atom attached to a Si atom close to the tetrahedral interstitial site. The defect has been studied by electron paramagnetic resonance,[2] deep level transient spectroscopy (DLTS),[3] optical absorption spectroscopy,[4] as well as theory.[5–10] The different structures of BI in the positive and negative charge states account for its negative-U character. The measured positions of the donor and acceptor levels[3] at $E_c-0.13$ eV and $E_c-0.37$ eV have been well reproduced by theory.[7,11] BI anneals out at around 240 K at a rate $\sim 10^7 \exp(-0.6\ \mathrm{eV}/kT)\ \mathrm{s}^{-1}$, suggesting an activation energy for migration of 0.6 eV.

Simultaneously with the anneal of BI, DLTS studies show the correlated growth of a level at $E_c-0.23$ eV.[12] There is evidence that this level belongs to the $\{B_i,O_i\}$ defect. Similar gap levels with identical annealing properties observed in other capacitance measurements on boron-doped irradiated Cz-Si have been attributed to the same boron-oxygen complex. DLTS studies by Mooney *et al.*[13] and other groups[14,15] have reported a B–O level at $E_c-0.27$ eV. Its introduction rate increases with the concentration of oxygen [O], and varies as $[B]^{1/2}$ or [B] at low concentrations,[13] and as $[B]^{-2}$ otherwise.[16] The high minority carrier capture cross section of this level, $\sigma_n=3\times10^{-13}$ cm^2 at 145 K, and the low majority carrier capture cross section of the order of $\sigma_p \sim 10^{-20}$ cm^2 suggest that the center is doubly positively charged before capturing the electron. The possibility of assignment to a second donor center was ruled out by the theoretical results of Adey *et al.*[17] who found a unique (0/+) level at $E_c-0.22$ eV. This level has also been placed at $E_c-0.30$ eV by Hall effect measurements,[18] and related to a 0.87 eV zero-phonon photoluminescence (PL) line.[19] From the spectral shape analysis and the temperature dependence of the PL peak, the level has been estimated to lie at $E_c-0.30$ and $E_c-0.26$ eV, respectively.

First-principles calculations[17] found that the ground-state structure of $\{B_i,O_i\}$ is that shown in Fig. 1(a). We label this configuration $\{B_i,O_i\}_a$. It has monoclinic-I (C_{1h}) symmetry, with a three-fold coordinated oxygen atom. The calculated binding energy relative to isolated B_i and O_i is 0.7 eV. Note that the structure is similar to that of the $\{C_i,O_i\}$ complex,[20] which has a much larger binding energy (1.7 eV).[11,20]

When adding the calculated binding energy of $\{B_i,O_i\}_a$ to the measured 0.6 eV migration barrier of BI,[12] one obtains a lower bound for the dissociation energy of 1.3 eV, remarkably close to the value of 1.2 eV measured by Mooney *et al.*[13] The calculated[17] (0/+) level of $\{B_i,O_i\}_a$ at $E_c-0.22$ eV was also close to the experimental values.

However, independent first-principles studies by Sanati *et al.*[21] found that structure $\{B_i,O_i\}_a$ is metastable with respect to the form shown in Fig. 1(b), which we label $\{B_i,O_i\}_b$. It contains a nearly substitutional boron atom (resembling the BI^+ defect) next to an interstitial oxygen. This complex also has C_{1h} symmetry, and a calculated binding energy of 0.47 eV.[21] A donor level for structure (b) was placed at $E_c-0.49$ eV. The different atomic arrangements imply that the local vibrational modes (LVMs) of $\{B_i,O_i\}_a$ differ in frequency and character from those of $\{B_i,O_i\}_b$. Unfortunately,

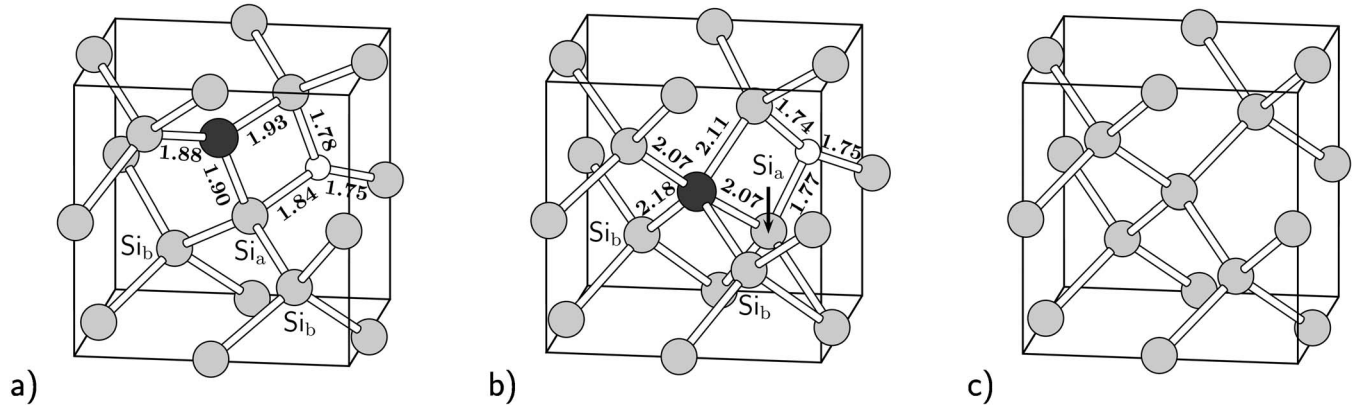

FIG. 1. Equilibrium structures of the $\{B_i,O_i\}$ defect: (a) $\{B_i,O_i\}_a$ and (b) $\{B_i,O_i\}_b$ and (c) conventional cell of Si to help the reader. Boron, oxygen, and silicon atoms are represented in black, white, and grey, respectively. Bond lengths are indicated in Å.

no vibrational spectroscopy data have been linked to either of the $\{B_i,O_i\}$ defect forms.

A comparison can be established with the case of another boron–oxygen complex, the substitutional boron-interstitial oxygen ($\{B_s,O_{2i}\}$) defect, which is responsible for the light-induced efficiency reduction of terrestrial solar cells *not* exposed to irradiation.[22–30] Sanati *et al.*[21] proposed a different lowest-energy configuration of this complex, 0.5 eV more stable than the square configuration previously proposed by Adey *et al.*[11,30] Recent experiments have shown that the decrease of the carrier lifetime attributed to this type of B–O complex proceeds via a two-step process:[25] (i) a rapid degradation step, which escaped detection in earlier studies and takes place during the first seconds or minutes, and (ii) a slow asymptotic decay-shaped stage. Both fast and slow processes exhibit the same dependence on the concentrations of B_s and O_i, and the same deactivation annealing temperature. However, the electronic properties and formation mechanisms of the defects involved in the two stages are distinct. This observation links well to the suggestion that the $\{B_s,O_{2i}\}$ defect is bistable.

Similarly, the existence of two closely related $\{B_i,O_i\}$ configurations with similar energies changes the way we understand interstitial-related reactions in *p*-doped Si. The carrier lifetime degradation and defect annihilation behavior may reveal additional features not discerned before. In this paper, the two theory groups involved in the earlier $\{B_i,O_i\}$ studies join efforts to predict the fundamental properties of the $\{B_i,O_i\}_a$ and $\{B_i,O_i\}_b$ defects. The predictions include the barrier between the two structures, electronic transitions, complete vibrational spectra, and the temperature dependence of the relative energies of the two defects in the 0 and +1 charge states.

II. METHOD

All calculations are carried out using first-principles density-functional packages, AIMPRO[31] and SIESTA,[32] within the local density approximation to the exchange-correlation potential (Refs. 33 and 34 for AIMPRO and Refs. 35 and 36 for SIESTA). The host crystal is represented by periodic supercells with 64 host atoms and a Monkhorst and Pack MP-2^3 special **k**-point scheme was used to sample the Brillouin zone.[37] Test calculations show that the use of a MP-4^3 special **k**-point grid does not produce relevant differences in the results. The zero-temperature energetics, electrical levels, and transformation barriers between the two structures are dealt with by using AIMPRO, whereas the complete vibrational spectra and vibrational free energies are investigated by using SIESTA.

The AIMPRO code replaces core states by the dual space separable pseudopotentials by Hartgwissen *et al.*,[38] whereas valence states are expanded over a set of atom-centered Cartesian-Gaussian functions. These consist of (4, 12, 12) independent *s*-, *p*-, and *d*-like functions centered on each Si atom. For O and B we use a total of 40 and 22 Gaussian basis functions, respectively. In the reciprocal space, a plane-wave basis set with a cutoff energy of 200 Ry was used. This method has been successful in previous studies of boron-oxygen defects in Si.[11,39]

The SIESTA calculations[40,41] use norm-conserving pseudopotentials in the Kleinman-Bylander form[42] to remove the core regions from the calculations. The basis sets for the valence regions are linear combinations of numerical atomic orbitals of the Sankey type,[43,44] generalized to be arbitrarily complete with the inclusion of multiple-zeta orbitals and polarization states.[40] In the present calculations, double-zeta (two sets of *s* and *p* orbitals) for the B and O atoms and polarized double-zeta (add one set of *d* orbitals) for the Si atoms are used. The charge density is projected on a real-space grid with an equivalent cutoff of 150 Ry to calculate the exchange-correlation and Hartree potentials.

The dynamical matrices are calculated at $\mathbf{k}=\Gamma$ using linear response theory.[45,46] The quality of the matrices obtained in this manner is now well documented.[47–50] In addition to providing all local and pseudolocal vibrational modes (LVMs and pLVMs, respectively), the knowledge of all normal modes of the cell allows the construction of the phonon density of states $g(\omega)$ and, therefore, of the Helmholtz vibrational free energy F_{vib}.[51] The calculation of the latter is straightforward once $g(\omega)$ is known. This function is obtained by evaluating the dynamical matrix at 90 **k** points in the Brillouin zone of the supercell. Note that $F_{\mathrm{vib}}(0\ \mathrm{K})$ is the total zero-point energy.

TABLE I. Calculated binding energies (eV) of $\{B_i,O_i\}_a$ and $\{B_i,O_i\}_b$. E_b^V and E_b^{tot} denote the binding energies determined when the zero-point energy is ignored or when it is taken into account, respectively.

	Code	$\{B_i,O_i\}_a^0$	$\{B_i,O_i\}_b^0$	$\{B_i,O_i\}_a^+$	$\{B_i,O_i\}_b^+$
E_b^V	AIMPRO	−0.70	−0.46	−0.70	−0.52
	SIESTA	−0.57	−0.47	−0.50	−0.47
E_b^{tot}	SIESTA	−0.53	−0.50	−0.45	−0.48

III. RESULTS

A. Energetics at $T=0$

Adey *et al.*[17] found that oxygen prefers to bind to a Si atom rather than directly to the B, and proposed the ground state $\{B_i,O_i\}_a$ shown in Fig. 1(a), where both B and O species are three-fold coordinated and form a four-fold ring in the (110) plane. On the other hand, the $\{B_i,O_i\}_b$ configuration, shown in Fig. 1(b), was obtained by Sanati *et al.*[21] This structure also has an oxygen atom bound to three Si atoms. However, the boron atom is at an almost substitutional site, pushing a Si atom close to the tetrahedral interstitial site. Both configurations have C_{1h} symmetry.

The binding energies $B_i^{0/+}+O_i^0 \rightarrow \{B_i,O_i\}^{0/+}-E_b$ have been calculated by using both SIESTA and AIMPRO from the energy of each species calculated in individual supercells. The calculated E_b is negative if the formation of the complex is energetically favorable. This calculation ignores the Madelung energy correction when calculating the energies of $\{B_i,O_i\}^+$ and B_i^+. However, this correction should be similar in both calculations, and therefore mostly cancel out when performing total energy differences.

The results obtained by using SIESTA and AIMPRO are summarized in Table I. The departure between the values obtained with both codes reflects the independence of the two calculations undertaken, and serves as an estimate to the calculational error.

Regardless of the method used, the bistability of the defect is evident. At $T=0$ K, and ignoring the total vibrational zero-point energy differences, structure $\{B_i,O_i\}_a$ is more stable than $\{B_i,O_i\}_b$ by 0.10–0.24 and 0.03–0.18 eV in the neutral and positive charged states, respectively. However, the two structures have different vibrational spectra (see Sec. III D). When zero point energies are included,[51] $\{B_i,O_i\}_b$ is more stable than $\{B_i,O_i\}_a$ by 0.03 eV in the + charge state, while $\{B_i,O_i\}_a$ remains more stable than $\{B_i,O_i\}_b$ but only by 0.03 eV in the 0 charge state.

B. Relative energies at finite temperatures

Since the $\{B_i,O_i\}$ defects form around room temperature, we also calculated the vibrational free energies of the two defects in both charge states, in order to check the relative stability of the defects at finite temperatures. The total energy E^{tot} is electronic energy, obtained from SIESTA, plus the vibrational free energy, calculated as described in Ref. 51. Since both structures have identical configurational entropies and almost identical electronic activities, the vibrational free energy is the only contribution that needs to be included. The total energy difference between the two structures $\Delta E = E^{tot}(\{B_i,O_i\}_a) - E^{tot}(\{B_i,O_i\}_b)$ is plotted as a function of temperature in Fig. 2 in the + and 0 charge states. The differences in electronic energy alone, which do not include zero-point energy differences, are marked on the vertical axis.

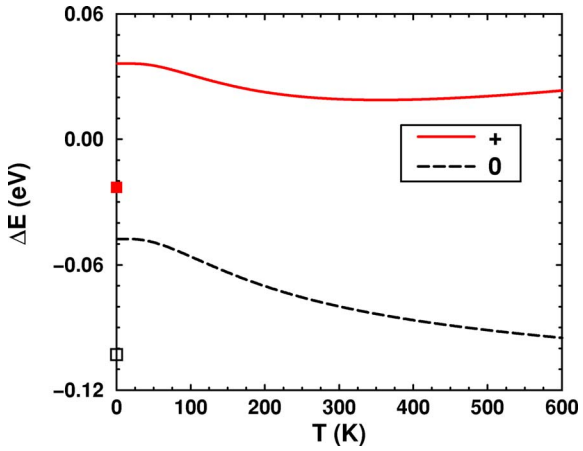

FIG. 2. (Color online) Temperature dependence of the electronic plus vibrational free energy difference between the $\{B_i,O_i\}_a$ and $\{B_i,O_i\}_b$ defects in the +1 (solid red line) and 0 (dashed black line) charge states. The solid (+1 charge state) and open (0 charge state) squares on the $T=0$ K axis show the total eletronic energy differences without zero-point energies.

At room temperature, the two structures of the defect are nearly degenerate in the + charge state (0.02 eV in favor of $\{B_i,O_i\}_b$). However, in the 0 charge state, we find that $\{B_i,O_i\}_a$ is the stable structure by a more substantial 0.08 eV. Assuming a Boltzmann distribution at room temperature, we get the following formation probabilities: 68% $\{B_i,O_i\}_b^+$ versus 32% $\{B_i,O_i\}_a^+$, and 95% $\{B_i,O_i\}_a^0$ versus 5% $\{B_i,O_i\}_b^0$.

C. Transformation barrier

The transformation barrier between the two structures was calculated using the improved tangent nudged elastic band (NEB) method.[52] The starting point of the diffusion calculation is the initial and final structures, $\mathbf{R}_A \equiv \mathbf{R}_0$ and $\mathbf{R}_B \equiv \mathbf{R}_N$. The initial chain of intermediate structures $\mathbf{R}_i$ with $i=1,\ldots,N-1$, called images, is generated by a linear extrapolation between the initial and final structures. Each pair of successive images is coupled by a virtual elastic band, and the atoms of each image are moved until the forces vanish. In the present calculations, we use a set of $N=5$ images. The same method and number of images was successfully used to calculate other diffusion barriers in silicon.[53]

Although the symmetry was not constrained during the diffusion simulation, the transformation proceeded in the (110) plane. One silicon atom in the position Si_a moves approximately along the [111] direction, away from its two Si neighbors, breaking the two Si_a-Si_b bonds (Fig. 1) and subsequently forming two new Si-Si bonds. Simultaneously, the

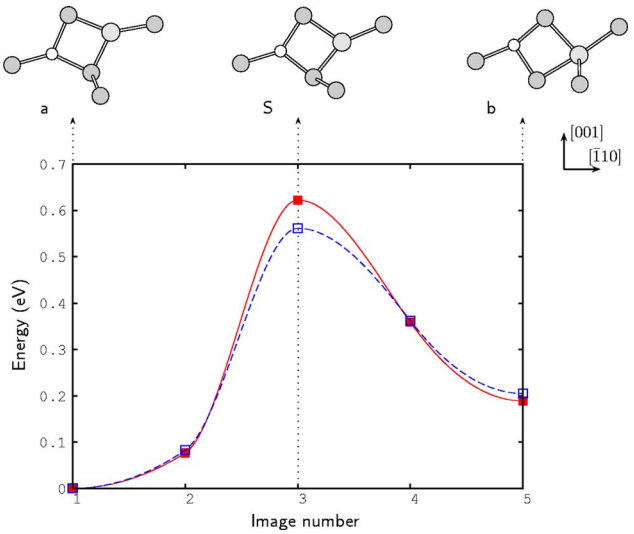

FIG. 3. (Color online) Minimum energy path for the transformation of $\{B_i,O_i\}_a$ into $\{B_i,O_i\}_b$. The zero-point energies are ignored in this calculation. The data for the positive and neutral charge states are represented by filled squares and empty squares, respectively. Energies are given with respect to $\{B_i,O_i\}_a$. Interpolation lines are added to help the visualization. Projections in the (110) plane of the equilibrium (a and b) and saddle point (S) structures are also shown. Silicon, boron, and oxygen atoms are represented in grey, light grey, and white, respectively.

boron atom moves along $\sim[00\bar{1}]$ toward the substitutional position forming new bonds with the Si_b atoms (Fig. 3).

The calculated energy barriers for the transformation $\{B_i,O_i\}_a \rightarrow \{B_i,O_i\}_b$ are 0.56 and 0.62 eV for the neutral and positively charged defects, respectively. These values neither consider zero-point energies nor any form of entropy contribution. Nevertheless, the barrier is sufficient to allow the coexistence of both structures at the temperature at which the B-O complexes form, ~240 K. In fact, the calculated transformation barrier is comparable to the activation energy for the diffusion of BI (experiment[12] 0.6 eV, theory[54] 0.4–0.7 eV) which is known to become mobile at about 230 K.[4,11]

We could not find a diffusion mechanism where $\{B_i,O_i\}$ diffuses as a single entity, without dissociating. It seems plausible that this defect would diffuse by a dissociative mechanism. It is possible that the BI unit resulting from the dissociation, or even other mobile BI defect would recapture the oxygen and thus promote its motion.

D. Local vibrational modes

The dynamical matrices of the supercells containing the two structures of $\{B_i,O_i\}$ have been calculated in both charge states using linear response theory for ^{11}B, O, and ^{28}Si. Their eigenvalues ω_s are the normal-mode frequencies and the orthonormal eigenvectors $e^s_{\alpha,i}$ give the displacement along the Cartesian direction i of atoms α in the mode s. Plots of $\Sigma_i(e^s_{B,i})^2$ and $\Sigma_i(e^s_{O,i})^2$ versus normal mode frequency (i.e., versus s) show the frequencies of the LVMs and pLVMs localized on the B and O atoms. Figure 4 shows these localization plots for the $\{B_i,O_i\}_a$ and $\{B_i,O_i\}_b$ defects in the 0 charge state, and Fig. 5 gives the same information in the +1 charge state.

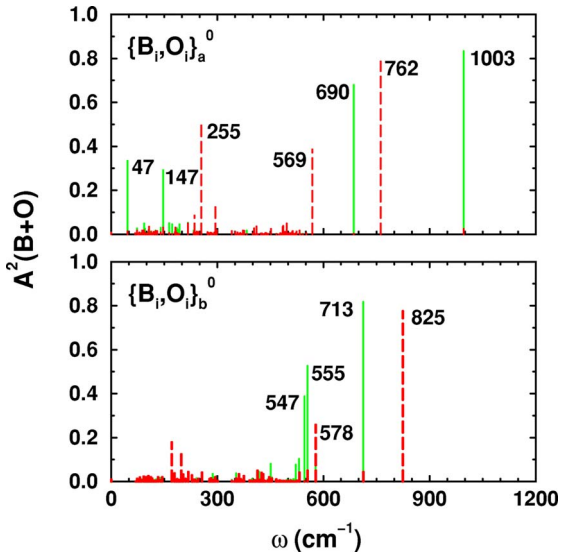

FIG. 4. (Color online) Relative amplitude of the B (solid green lines) and O (dashed red lines) oscillations versus normal mode frequency for the neutral $\{B_i,O_i\}_a$ (top) and $\{B_i,O_i\}_b$ (bottom) defects. The frequencies of the more strongly localized modes are given.

The modes are described and the frequencies for various isotope substitutions are given in Ref. 39 for $\{B_i,O_i\}_a$ and Ref. 55 for $\{B_i,O_i\}_b$. In both charge states, the highest-frequency LVM for the $\{B_i,O_i\}_a$ defect is associated with B, while it is an O-related mode in the case of the $\{B_i,O_i\}_b$ defect.

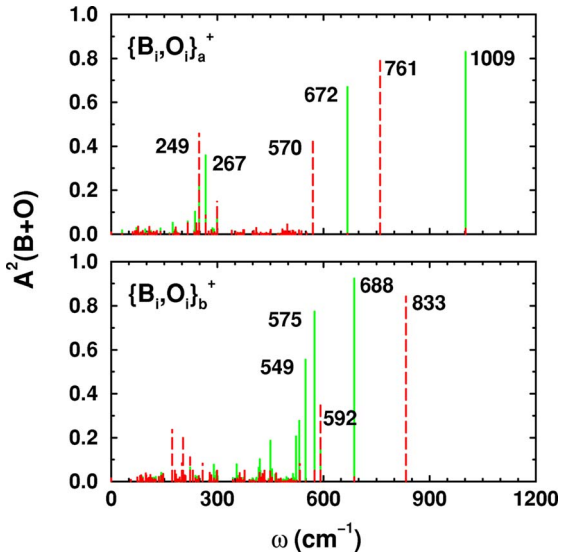

FIG. 5. (Color online) Relative amplitude of the B (solid green lines) and O oscillations (dashed red lines) versus normal mode frequency for the $\{B_i,O_i\}_a$ (top) and $\{B_i,O_i\}_b$ (bottom) defects in the +1 charge state. The frequencies of the more strongly localized modes are given.

TABLE II. Calculated acceptor and donor levels [(−/0) and (0/+)] for the $\{B_i,O_i\}$ defects using B_i and $\{C_i,O_i\}$ as marker defects. All the values are in eV. Zero-point energies are not taken into account. The measured values of the electric levels assigned with the $\{B_i,O_i\}$ defect range from 0.23–0.30 eV.

Level	$E(-/0)$	$E(0/+)$	
Marker	B_i	B_i	C_iO_i
Marker level	$E_c-0.37$[a]	$E_c-0.13$[a]	$E_v+0.38$[b]
$\{B_i,O_i\}_a$	$E_c-0.07$	$E_c-0.12$	$E_v+0.91$
			$\simeq E_c-0.26$
$\{B_i,O_i\}_b$	$E_c-0.13$	$E_c-0.08$	$E_v+0.97$
			$\simeq E_c-0.20$

[a]See Ref. 3.
[b]See Ref. 13.

E. Electric levels

The electric levels were calculated using the marker method.[56] The position of donor (acceptor) level of a defect $E_D(q/q+1)$ relative to the valence band (conduction band), can be estimated from the difference between the total energies of the relaxed, positively (negatively) charged, and neutral defects, $\Delta E_D(q/q+1)=E_D(q)-E_D(q+1)$. We can then compare $\Delta E_D(q/q+1)$ with the analogous quantity found for a standard defect designated *marker*:

$$E_D(q/q+1)-E_M(q/q+1)=\Delta E_D(q/q+1)-\Delta E_M(q/q+1).$$

The marker should be a defect with known donor or acceptor levels. The accuracy of the method is enhanced when: (i) The electric level of the marker is close to the defect under study, and (ii) the wave function of the state associated with the donor/acceptor level is similar in form and extent for both the marker and defect under scrutiny.

Under these circumstances, we selected B_i and $\{C_i,O_i\}$ as marker defects. Both are well known defects and their electrical levels have been established by capacitance measurements[3,13] and supported by theory.[7,11,20,57] B_i has an acceptor level at $E_c-0.13$ eV,[3] (close to the position where we expect to find the acceptor level of both $\{B_i,O_i\}$ defects) and, when positively charged, also has a similar structure to $\{B_i,O_i\}$.

Despite possessing a donor level in the lower part of the band gap, the $\{C_i,O_i\}$ center is remarkably similar to $\{B_i,O_i\}_a$. They possess very similar donor states in the gap. In both defects, the donor state is a strongly localized *p*-like orbital centered on the carbon and boron atoms, respectively.

The calculated thermodynamic levels are shown in Table II. It is instructive to calculate the energy separation between the donor levels of the two markers. The comparison of the calculated ionization energies holds $E(0/+)_{C_i,O_i}-E(0/+)_{B_i}=0.52$ eV, while the difference between the measured values (if we take the band gap to be 1.17 eV) is $1.17-0.13-0.38=0.66$ eV; i.e., 0.14 eV larger. This gives us an estimate of the error involved in this calculation.

The calculated electric levels reported in Table II are direct transitions involving no structural modification. If zero-point energies are included, though, the thermodynamic level is defined by the lower-energy structures which are $\{B_i,O_i\}_a$ in the neutral charge state and $\{B_i,O_i\}_b$ in the positive charge state. Nevertheless, the vertical transitions are expected to be observed in the DLTS measurements if, at the temperature of measurement (about 100 K),[12] the structural change does not occur. In any case, note that the difference between zero-point energies is small compared with the calculation error associated with the electric levels.

A donor level in the upper part of the band gap has been identified with the $\{B_i,O_i\}$ defect but, as mentioned in Sec. I, the measured values range from $E_c-0.23$ to $E_c-0.30$ eV (Refs. 12–19) depending on the author and technique used. The $E(0/+)$ levels calculated using $\{C_i,O_i\}$ as a marker are placed at $E_c-0.26$ and $E_c-0.20$ eV, very close to some of the measured values. We also find acceptor levels (−/0), but these are very close to the conduction band and within the precision of our method could still be situated outside the forbidden band gap.

The existence of double donor levels was investigated as well. In this case, it is difficult to find a suitable marker because most of the point defect double donors in Si are substitutional impurities. This is the case of substitutional sulphur. Using this marker, we obtain the rough estimates of $E_c-1.22$ and $E_c-1.10$ eV for $\{B_i,O_i\}_a$ and $\{B_i,O_i\}_b$, respectively. This does not rule out the existence of a second donor level, although should there be one, it is very close to the valence band and, consequently, not identifiable with the defect observed by Mooney *et al.*[13]

Our values are also in reasonable agreement with previous calculations that placed the donor level of $\{B_i,O_i\}_a$ at $E_c-0.22$ eV (using bulk Si as a marker) (Ref. 11) and that of $\{B_i,O_i\}_b$ at $E_c-0.49$ eV (using interstitial carbon as a marker).[21] However, the present direct comparison allows us to locate the donor level of $\{B_i,O_i\}_b$ closer to the bottom of the conduction band.

Although the difference between the values found in literature can be attributed to the methods used and subtle differences in the measured quantities, the existence of two alternative structures with close energies in the two charge states makes us question whether more than a single transition is being observed.

IV. CONCLUSIONS

We have investigated the properties of two alternative forms of the interstitial boron-interstitial oxygen complex, labeled $\{B_i,O_i\}_a$ and $\{B_i,O_i\}_b$, initially suggested by Adey *et al.* and Sanati *et al.*, respectively.[17,21,30] Although these two models had previously been reported independently in the literature, the present study presents a comparative study that bridges the work of both groups.

If the vibrational zero-point energy is ignored, $\{B_i,O_i\}_a$ is slightly more stable in the neutral and postive charge states than $\{B_i,O_i\}_b$. However, if this contribution is included, the energy difference between the two structures becomes smaller and $\{B_i,O_i\}_b$ is slightly more stable than $\{B_i,O_i\}_b$ in the positive charge state. At room temperature, populations

of the $\{B_i, O_i\}_a$ and $\{B_i, O_i\}_b$ forms are quite different, especially in the 0 charge state.

The NEB method was employed to calculate the transformation barrier between the two structures, yielding an activation energy of about 0.6 eV for both charge states. These two lines of evidence indicate that, at the temperature of formation of the observed interstitial boron-interstitial oxygen complexes (240 K), both species may be present. The calculated electric levels of the two structures are close to the range of experimental values reported by various groups. Nevertheless, the presence of two variants of the defect could be verified by vibrational spectroscopy, since the LVMs arising from both structures are very distinct.

The coexistence of these two forms of interstitial boron-interstitial oxygen complexes implies that the behavior of the radiation-induced lifetime degradation of Cz-Si solar cells may possess complex features not revealed so far.

ACKNOWLEDGMENTS

The work of one of the authors (S.K.E.) is supported in part by the National Renewable Energy Laboratory and the R. A. Welch Foundation. Another author (A.C.) acknowledges the Portuguese foundation *Fundacão para a Ciência e para a Tecnologia* for financial support.

*Electronic address: carvalho@excc.ex.ac.uk

[1] I. Weinberg, S. Mehta, and C. K. Swartz, Appl. Phys. Lett. **44**, 1071 (1984).
[2] G. D. Watkins, Phys. Rev. B **12**, 5824 (1975).
[3] R. D. Harris, J. L. Newton, and G. D. Watkins, Phys. Rev. B **36**, 1094 (1987).
[4] A. K. Tipping and R. C. Newman, Semicond. Sci. Technol. **2**, 389 (1987).
[5] E. Tarnow, Europhys. Lett. **16**, 449 (1991).
[6] J. Zhu, Comput. Mater. Sci. **12**, 309 (1998).
[7] M. Hakala, M. J. Puska, and R. M. Nieminen, Phys. Rev. B **61**, 8155 (2000).
[8] J.-W. Jeong and A. Oshiyama, Phys. Rev. B **64**, 235204 (2001).
[9] J. Adey, J. P. Goss, R. Jones, and P. R. Briddon, Physica B **340**, 505 (2003).
[10] P. Deák, A. Gali, A. Sólyom, P. Ordejón, K. Kamarás, and G. Battistig, J. Phys.: Condens. Matter **15**, 4967 (2003).
[11] J. Adey, Ph.D. thesis, University of Exeter, 2004, and references therein.
[12] J. R. Troxell and G. D. Watkins, Phys. Rev. B **22**, 921 (1980).
[13] P. M. Mooney, L. J. Cheng, M. Süli, J. D. Gerson, and J. W. Corbett, Phys. Rev. B **15**, 3836 (1977).
[14] S. Zhao, A. M. Agarwal, J. L. Benton, G. H. Gilmer, and L. C. Kimerling, in *Defects in Electronic Materials II*, edited by J. Michel, T. Kennedy, K. Wada, and K. Thonke [Mater. Res. Soc. Symp. Proc. **442**, 231 (1997)].
[15] P. J. Drevinsky, C. E. Caefer, S. P. Tobin, J. C. Mikkelsen Jr., and L. C. Kimerling, Mater. Res. Soc. Symp. Proc. **104**, 167 (1988).
[16] L. C. Kimerling, M. T. Asom, J. L. Benton, P. J. Drevinsky, and C. E. Caefer, Mater. Sci. Forum **38**, 141 (1989).
[17] J. Adey, R. Jones, and P. R. Briddon, Appl. Phys. Lett. **83**, 665 (2003).
[18] H. Matsuura, Y. Uchida, N. Nagai, T. Hisamatsu, T. Aburaya, and S. Matsuda, Appl. Phys. Lett. **76**, 2092 (2000).
[19] M. Tajima, M. Warashina, T. Hisamatsu, and S. Matsuda, IEEE Trans. Nucl. Sci. **48**, 2127 (2001).
[20] J. Coutinho, R. Jones, P. R. Briddon, S. Öberg, L. I. Murin, V. P. Markevich, and J. L. Lindström, Phys. Rev. B **65**, 014109 (2001).
[21] M. Sanati and S. K. Estreicher, Phys. Rev. B **72**, 165206 (2005).
[22] J. Schmidt and A. Cuevas, J. Appl. Phys. **86**, 3175 (1999).
[23] J. Schmidt and K. Bothe, Phys. Rev. B **69**, 024107 (2004).
[24] J. Schmidt, Appl. Phys. Lett. **82**, 2178 (2003).
[25] K. Bothe and J. Schmidt, J. Appl. Phys. **99**, 013701 (2006).
[26] J. Schmidt, K. Bothe, and R. Hezel, Appl. Phys. Lett. **80**, 4395 (2002).
[27] S. Rein and S. W. Glunz, Appl. Phys. Lett. **82**, 1054 (2003).
[28] D. Macdonald, P. N. K. Deenapanray, A. Cuevas, S. Diez, and S. W. Glunz, Solid State Phenom. **108**, 497 (2005).
[29] S. W. Glunz, S. Rein, W. Warta, J. Knobloch, and W. Wettling, *Proceedings of the Second World Conference on Photovoltaic Energy Conversion* (European Commission, Ispra, 1998), p. 1343.
[30] J. Adey, R. Jones, D. W. Palmer, P. R. Briddon, and S. Öberg, Phys. Rev. Lett. **93**, 055504 (2004).
[31] P. R. Briddon and R. Jones, Phys. Status Solidi B **217**, 131 (2000).
[32] J. M. Soler, E. Artacho, J. D. Gale, A. García, J. Junquera, P. Ordejón, and D. Sánchez-Portal, J. Phys.: Condens. Matter **14**, 2745 (2002).
[33] S. Goedecker, M. Teter, and J. Hutter, Phys. Rev. B **54**, 1703 (1996).
[34] J. P. Perdew and Y. Wang, Phys. Rev. B **45**, 13244 (1992).
[35] D. M. Ceperley and B. J. Alder, Phys. Rev. B **45**, 566 (1980).
[36] J. P. Perdew and A. Zunger, Phys. Rev. B **23**, 5048 (1981).
[37] H. J. Monkhorst and J. D. Pack, Phys. Rev. B **13**, 5188 (1976).
[38] C. Hartwigsen, S. Goedecker, and J. Hutter, Phys. Rev. B **58**, 3641 (1998).
[39] A. Carvalho, R. Jones, J. Coutinho, and P. R. Briddon, J. Phys.: Condens. Matter **17**, L155 (2005).
[40] D. Sánchez-Portal, P. Ordejón, E. Artacho, and J. M. Soler, Int. J. Quantum Chem. **65**, 453 (1997).
[41] E. Artacho, D. Sánchez-Portal, P. Ordejón, A. García, and J. M. Soler, Phys. Status Solidi B **215**, 809 (1999).
[42] L. Kleinman and D. M. Bylander, Phys. Rev. Lett. **48**, 1425 (1982).
[43] O. F. Sankey and D. J. Niklewski, Phys. Rev. B **40**, 3979 (1989); O. F. Sankey, D. J. Niklewski, D. A. Drabold, and J. D. Dow, *ibid.* **41**, 12750 (1990).
[44] A. A. Demkov, J. Ortega, O. F. Sankey, and M. P. Grumbach, Phys. Rev. B **52**, 1618 (1995).
[45] S. Baroni, P. Giannozzi, and A. Testa, Phys. Rev. Lett. **58**, 1861 (1987).
[46] X. Gonze and C. Lee, Phys. Rev. B **55**, 10355 (1997).

[47] J. M. Pruneda, S. K. Estreicher, J. Junquera, J. Ferrer, and P. Ordejón, Phys. Rev. B **65**, 075210 (2002).
[48] M. Sanati, S. K. Estreicher, and M. Cardona, Solid State Commun. **131**, 229 (2004); R. K. Kremer, M. Cardona, E. Schmitt, J. Blumm, S. K. Estreicher, M. Sanati, M. Bockowski, I. Grzegory, T. Suski, and A. Jezowski, Phys. Rev. B **72**, 075209 (2005).
[49] S. K. Estreicher, D. West, J. Goss, S. Knack, and J. Weber, Phys. Rev. Lett. **90**, 035504 (2003).
[50] S. K. Estreicher, D. West, and M. Sanati, Phys. Rev. B **72**, 121201(R) (2005).
[51] S. K. Estreicher, M. Sanati, D. West, and F. Ruymgaart, Phys. Rev. B **70**, 125209 (2004).
[52] G. Henkelman and H. Jónsson, J. Chem. Phys. **113**, 9978 (2000).
[53] N. Fujita, R. Jones, J. P. Goss, P. R. Briddon, T. Frauenheim, and S. Öberg, Appl. Phys. Lett. **87**, 021092 (2005).
[54] W. Windl, M. M. Bunea, R. Stumpf, S. T. Dunham, and M. P. Masquelier, Phys. Rev. Lett. **83**, 4345 (1999).
[55] M. Sanati and S. K. Estreicher, Physica B **376-377**, 133 (2006).
[56] A. Resende, R. Jones, S. Öberg, and P. R. Briddon, Phys. Rev. Lett. **82**, 2111 (1999).
[57] P. Deák, A. Gali, A. Sólyom, A. Buruzs, and T. Frauenheim, J. Phys.: Condens. Matter **17**, S2141 (2005).